



# Nanosponges by the oxo-Michael polyaddition of cyclodextrins as sorbents of water pollutants: the *o*-toluidine case

Valentina Pifferi<sup>1</sup> · Elena Ferrari<sup>1</sup> · Amedea Manfredi<sup>1</sup> · Paolo Ferruti<sup>1</sup> · Jenny Alongi<sup>1</sup> · Elisabetta Ranucci<sup>1</sup> · Luigi Falciola<sup>1</sup>

Received: 9 May 2022 / Accepted: 8 August 2022  
© The Author(s) 2022

## Abstract

Hydrophilic cyclodextrin nanosponges were prepared by the oxo-Michael polyaddition in an aqueous solution at pH > 10 of  $\alpha$ -,  $\beta$ -, and  $\gamma$ -cyclodextrin with 1,4-bisacryloylpiperazine or 2,2-bisacrylamidoacetic acid. These nanosponges and, for comparison purposes, their precursor cyclodextrins were tested as sorbents of *o*-toluidine, a carcinogenic wastewater contaminant, by monitoring the depletion of *o*-toluidine from a  $10^{-4}$  M (10 ppm) aqueous solutions. To this aim, an innovative analytical procedure was used: The voltammetric peak currents of *o*-toluidine in linear sweep voltammetry experiments were registered using multi-walled carbon nanotubes-modified glassy carbon electrodes. The experimental sorption curves fitted a mono-exponential kinetic model, and the residual *o*-toluidine was 0.16 ppm, one order of magnitude lower than those of all other sorbents reported so far. The sorption capacities ranged from 88 to 199  $\mu\text{mol g}^{-1}$  (10–21.3  $\text{mg g}^{-1}$ ), equal to or higher than those of the parent cyclodextrins. All nanosponges were completely regenerated by extracting with methanol. After regeneration, the sorption capacity slightly improved, suggesting a rearrangement of the nanosponge network. Overall, it may be reasonably concluded that the cyclodextrin nanosponges reported in this paper warrant potential as *o*-toluidine exhaustive sorbents.

**Keywords** Cyclodextrin nanosponges · 1,4-Bisacryloylpiperazine · 2,2-Bisacrylamidoacetic acid · *o*-Toluidine sorption in water · Voltammetric detection

## Introduction

*o*-Toluidine is an important organic intermediate used, *inter alia*, in the production of dyes, synthetic rubber, chemicals, and, as a curing agent, epoxy resins. In addition, it is a major

component of tobacco smoke (OECD 2004) and, consequently, ubiquitous in the human environment. *o*-Toluidine manufacturing and processing have produced increasing amounts of toluidine-polluted wastewaters, eventually merging into water bodies. *o*-Toluidine is classified by the International Agency for Research on Cancer (IARC) as “carcinogenic to humans” (group 1) (Baan et al. 2008); therefore, its efficient removal from water is required. Different technologies are currently available to remove *o*-toluidine from wastewater, including photodegradation (Cappelletti et al. 2015; Pifferi et al. 2015; San and Çjnar 2016), electrochemical treatment (López-Grimau et al. 2013), oxidation (Anotai et al. 2011), microbial digestion (Liu et al. 2002), and adsorption. Among them, adsorption is reckoned as one of the most attractive and effective purification techniques in wastewater treatment. Various sorbents have been reported in the literature (Elgarahy et al. 2021; El-Sayed et al. 2019) and in particular for anilines, including *o*-toluidine, such as organoclay (Bishop et al. 2002; Zhang and Sparks 1993), montmorillonite (Essington 1994), silica (Voumard et al. 1995), rubber tire (Gupta et al. 2012), zeolites (Titus et al. 2002), activated carbon

Responsible Editor: George Z. Kyzas

## Highlights

- Hydrophilic cyclodextrin nanosponges by oxo-Michael polyaddition in H<sub>2</sub>O solution.
- Nanosponges can sorb *o*-toluidine, a carcinogenic wastewater contaminant.
- Residual *o*-toluidine at 0.16 ppm, one order magnitude lower than other sorbents.
- Experimental sorption curves fitted a mono-exponential kinetic model.
- Innovative electroanalytical procedure used for *o*-toluidine detection.

✉ Luigi Falciola  
luigi.falciola@unimi.it

<sup>1</sup> Dipartimento Di Chimica, Università Degli Studi Di Milano, via C. Golgi 19, 20133 Milano, Italy

in powder, granular, or fiber form (Duman and Ayranci 2005) and polymers (Jianguo et al. 2005).

Cyclodextrins (CDs) are cyclic oligosaccharides formed by 6 ( $\alpha$ -CD), 7 ( $\beta$ -CD), or 8 ( $\gamma$ -CD) glucopyranose units. They are well known to possess a hydrophobic cavity forming inclusion complexes with organic molecules through host-guest interactions, with dimensional selectivity due to the different sizes of their inner cavity (Dodziuk 2006; Szejtli 1998). CD-containing polymers, either linear (Janus et al. 1999) or immobilized on solid supports (Allabashi et al. 2007; Fan et al. 2003; Faraji et al. 2011) or crosslinked CD resins (Crini et al. 1999; García-Zubiri et al. 2007; Romo et al. 2008; Wilson et al. 2011; Yamasaki et al. 2006; Yu et al. 2003) were extensively studied as sorbents of organic pollutants with removal efficacy ranging within ample limits (Crini 2005, Yadav et al. 2022). Since the late nineties, hyper-crosslinked CDs have commonly been referred to as nanosponges (Ahmed et al. 2013; Li and Ma 1999). Nanosponges are supramolecular cage-like architectures in which the CD units are connected by many short moieties forming nanochannels (Bilensoy 2011; Krabicov et al. 2020; Mhlanga et al. 2007; Petitjean et al. 2021; Rizzi et al. 2021; Sherje et al. 2017; Taka et al. 2017; Trotta et al. 2012; Varana et al. 2020). Nanosponges are nanoporous by definition and show high inclusion constants with many organic pollutants, including aromatic and chlorinated compounds (Berto et al. 2007a and 2007b; Gupta et al. 2012; Sun et al. 2010; Rizzi et al. 2021; Yadav et al. 2022). Most nanosponges are based on  $\beta$ -CD, the cheapest CD on the market, and only a few examples of  $\alpha$ - and  $\gamma$ -CD nanosponges have been reported (Cavalli et al. 2010). Nanosponges were obtained by interconnecting the CD molecules with different crosslinking agents, such as  $N,N'$ -carbonyldiimidazole (Ansari et al. 2011), triphosgene (Trotta 2011), diphenyl carbonate (Swaminathan et al. 2013), or organic dianhydrides (Mognetti et al. 2021). For all of them, the coupling reactions demanded organic solvents. Subsequently,  $\beta$ -CD-based nanosponges were synthesized in water at pH > 12 by the Michael oxo-polyaddition of  $\beta$ -CD, or  $\beta$ -CD/2-methylpiperazine mixtures, with 2,2-bisacrylamidoacetic acid (Swaminathan et al. 2010). Under these conditions,  $\beta$ -CD acted as a multifunctional monomer and gave rise to a previously undescribed type of nanosponges. In the present work, this preparation method was extended to  $\alpha$ - and  $\gamma$ -CD, and a small library of CD nanosponges was prepared by polyaddition of all three CD's with either 1,4-bisacryloylpiperazine or 2,2-bisacrylamidoacetic acid. These nanosponges were then tested as sorbents to remove *o*-toluidine from water and compared in this regard with their CD precursors. *o*-Toluidine sorption was monitored by using a previously optimized electroanalytical method

based on linear sweep voltammetry (LSV) at multi-walled carbon nanotubes-modified glassy carbon electrode (Mardegan et al. 2014; Pifferi et al. 2014). The accuracy, sensitivity, and robustness of this optimized method were already demonstrated in previous papers on the degradation of *o*-toluidine (Cappelletti et al. 2015; Pifferi et al. 2015).

## Experimental

### Materials

Solvents and reagents, unless otherwise indicated, were analytical-grade commercial products and used as received considering the grade declared by the dealer.  $\alpha$ -Cyclodextrin ( $\alpha$ -CD) (89.5%) was purchased from Alfa Aesar,  $\beta$ -cyclodextrin ( $\beta$ -CD) (95%) from Fluka and  $\gamma$ -cyclodextrin ( $\gamma$ -CD) (97%) from ABCR. Lithium hydroxide monohydrate ( $\text{LiOH}\cdot\text{H}_2\text{O}$ ) (99%), ethanol (>99.8%), and methanol (99%) were purchased from Sigma Aldrich. 2,2-Bisacrylamidoacetic acid (BAC) and 1,4-bisacryloylpiperazine (BP) were prepared as previously reported (Ferruti et al. 1999; Ferruti 1985). Distilled water (18 M $\Omega$  cm) purified with a Millipore Milli-Q apparatus was used in all experiments.

### Synthesis of CD-bisacrylamide nanosponges

#### Synthesis of BAC-based CD nanosponges

In a typical procedure, a solution of  $\alpha$ -CD (3.125 g, 2.9 mmol) and  $\text{LiOH}\cdot\text{H}_2\text{O}$  (0.357 g, 8.4 mmol) in water (1.9 mL) was mixed with an aqueous solution of BAC (2.135 g, 10.6 mmol) and  $\text{LiOH}\cdot\text{H}_2\text{O}$  (0.445 g, 10.6 mmol) in 2.2 mL water. The mixture was allowed to react for 24 h at 25 °C. The final product appeared as a homogeneous, transparent, and soft nanosponge, which was first soaked for 2 h in 50 mL deionized water, allowed for swelling for a further 2 h, brought to pH 5 with 37% HCl, and soaked for 2 h in ethanol (50 mL). This extracting procedure was repeated three times. The extracted product was finally dried to constant weight. Yield: 5.26 g (69%).

BAC- $\beta$ -CD and BAC- $\gamma$ -CD were prepared similarly. The reagents used in the preparation of all BAC nanosponges and their amounts were as follows.

Synthesis of BAC- $\beta$ -CD nanosponges:  $\beta$ -CD (3.674 g, 3.1 mmol),  $\text{LiOH}\cdot\text{H}_2\text{O}$  (0.389 g, 9.2 mmol),  $\text{H}_2\text{O}$  (2.4 mL), BAC (1.887 g, 9.4 mmol),  $\text{LiOH}\cdot\text{H}_2\text{O}$  (0.396 g, 9.4 mmol),  $\text{H}_2\text{O}$  (1.8 mL). Yield: 76.2% (3.76 g).

Synthesis of BAC- $\gamma$ -CD nanosponges:  $\gamma$ -CD (3.607 g, 2.7 mmol),  $\text{LiOH}\cdot\text{H}_2\text{O}$  (0.554 mg, 13.1 mmol),  $\text{H}_2\text{O}$  (2.7 mL), BAC (1.347 g, 6.7 mmol),  $\text{LiOH}\cdot\text{H}_2\text{O}$  (0.285 mg, 6.7 mmol),  $\text{H}_2\text{O}$  (1.2 mL). Yield: 47.4% (4.96 g).

## Synthesis of BP-based CD nanosponges

BP- $\alpha$ -CD and BP- $\beta$ -CD were prepared following the same procedure described for BAC- $\alpha$ -CD by substituting BP for equimolar amounts of BAC, apart from the fact that BP was dissolved in plain water before mixing with the CD/LiOH solution. The same reaction performed with  $\gamma$ -CD failed to produce insoluble crosslinked nanosponges. In detail, the reagents and amounts used were as follows:  $\alpha$ -CD (3.125 g, 2.9 mmol), LiOH•H<sub>2</sub>O (0.235 g, 5.5 mmol), H<sub>2</sub>O (1.7 mL), BP (2.072 g, 10.7 mmol), H<sub>2</sub>O (1.9 mL). Yield: 52% (5.20 g).

BP- $\beta$ -CD nanosponges were prepared similarly using the following reagent amounts:  $\beta$ -CD (3.674 g, 3.1 mmol), LiOH•H<sub>2</sub>O (0.375 g, 8.9 mmol), H<sub>2</sub>O (2.2 mL), BP (1.795 g, 9.25 mmol), H<sub>2</sub>O (1.7 mL). Yield: 47.4% (5.50 g).

## Characterization of CD nanosponges

### Elemental analysis

Elemental analyses were performed by the Analytical Laboratory of the Polytechnic University of Milano, Italy, using a Mettler Toledo Elemental Analyzer.

### FTIR analysis

The FTIR spectra were collected on solid samples dispersed in KBr pellets using a Perkin Elmer 100 spectrometer, as the average of 16 individual scans at 2 cm<sup>-1</sup> resolution in the 4000–600 cm<sup>-1</sup> interval and with corrections for atmospheric water and carbon dioxide.

### Swelling tests

Dry finely ground samples (30 mg) were suspended in ethanol (7 mL) and allowed to settle. The supernatant liquid was then carefully removed and the solid suspended three times in either water or 0.01 M PBS pH 7.4, gently shaken for 15 min, and then allowed to settle. Finally, the swelling degree (SD) was evaluated at equilibrium using Eq. (1):

$$SD(\%) = \frac{V_t}{V_{t0}} \cdot 100 \quad (1)$$

where  $V_t$  is the volume of the swollen nanosponge at equilibrium and  $V_{t0}$  is the volume of the dry sample.

### Thermal analyses

Differential scanning calorimetry (DSC) analyses were performed with a heat flux Mettler Toledo DSC823 calorimeter

on 10 mg samples sealed in standard aluminum pans under a 20 mL min<sup>-1</sup> nitrogen flow and with a 20 °C min<sup>-1</sup> heating/cooling rate. Empty pans were used as references. The analyses consisted of first heating run from 25 to 200 °C, followed by a cooling run from 200 to 25 °C and second heating run from 25 to 300 °C. Thermogravimetric (TG) analyses were performed with a Perkin Elmer TGA analyzer 4000 on 10 mg samples, in the 30–600 °C range, under a 50 mL min<sup>-1</sup> nitrogen flow and with a 20 °C min<sup>-1</sup> heating rate.

## Assessment of the *o*-toluidine sorption ability of CD nanosponges

### *o*-Toluidine detection

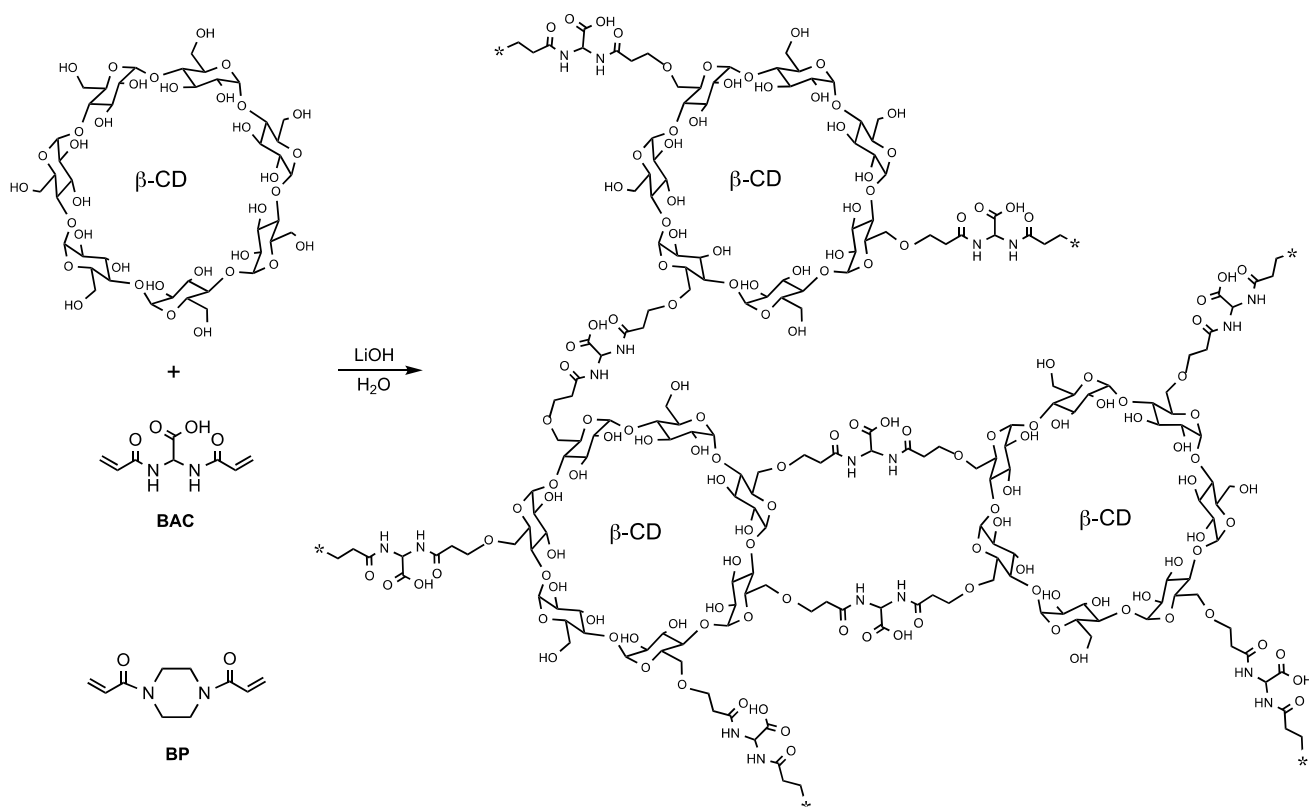
All experiments were carried out using an Autolab PG-Stat 12 (Ecochemie, the Netherlands) potentiostat/galvanostat, according to a previously optimized method (Pifferi et al. 2014). The voltammetric cell was conical (5 mL operating volume), including an Ag/AgCl/saturated KCl electrode as a reference, a Pt wire as a counter, and a multi-walled carbon nanotubes (MWCNT)-modified glassy carbon (GC) electrode as working electrodes, respectively. The GC electrode surface was initially cleaned with synthetic diamond powder (Aldrich, diameter 1  $\mu$ m) on a Struers DP Nap wet cloth. Subsequently, 20  $\mu$ L of a suspension of MWCNT in dimethylformamide (0.5 mg mL<sup>-1</sup>) was deposited on a glassy carbon electrode and dried at 25 °C until complete evaporation of the casting solvent.

The working cell was thoroughly cleaned with nitric acid and ultrapure water (MilliQ<sup>®</sup> Millipore) before each experiment. The sorption kinetics was assessed by monitoring the corresponding voltammetric peak currents during linear sweep voltammetry (LSV) experiments. To each sample of sorption solution (0.6 mL), 0.6 mL of 0.2 M HCl (ultrapure Fluka) was added as a supporting electrolyte before measurement. Voltammograms were recorded from the lowest concentration to the highest one. Peak heights were obtained after background subtraction.

### Assessment of *o*-toluidine sorption ability

The ability to sorb *o*-toluidine from the CD nanosponges and the parent soluble  $\alpha$ -,  $\beta$ -, and  $\gamma$ -CDs was determined by monitoring *o*-toluidine depletion from an aqueous solution of 10<sup>-4</sup> M (10 ppm) in batch reactors under slight magnetic stirring. The selected starting concentration of *o*-toluidine was one order of magnitude higher than the UK maximum exposure limit (Gregg et al. 1998).

As regards  $\alpha$ -,  $\beta$ -, and  $\gamma$ -CDs, the sorbent (30 mg) was dissolved in 100 mL 10<sup>-4</sup> M *o*-toluidine solution. As regards nanosponges, the sorbent (30 mg) was put in a small punctured paper bag (tea bag) and subsequently inserted in 100



**Scheme 1** Synthesis of BAC-CD and BP-CD nanosponges. As an example, the structure of the reaction product of  $\beta$ -CD with BAC is shown in detail

mL  $10^{-4}$  M *o*-toluidine solution. This procedure allowed a facile sorbent separation from the decontaminated water at the end of the experiment.

#### Nanosponge regeneration after *o*-toluidine sorption

The *o*-toluidine-loaded samples (30 mg) were soaked in 70:30 methanol/water (20 mL) and shaken for 20 min. The sorbent was then recovered, thoroughly rinsed with water to completely remove methanol, and finally re-used for *o*-toluidine sorption. The sorption–desorption cycles were repeated twice.

## Results and discussion

### Synthesis of CD nanosponges

The synthetic procedure adopted for preparing CD nanosponges involved the activation of the CD hydroxyl groups by deprotonation in water at pH  $\geq 12$  (Scheme 1). Under these conditions,  $\alpha$ - and  $\beta$ -CD's behaved as multifunctional monomers giving crosslinked resins (i.e., nanosponges) by one-pot polyaddition with bisacrylamides. No additional

solvents or catalysts were added. A neutral bisacrylamide (1,4-bis(acryloyloxy)piperazine, BP) and a strongly acidic carboxylated bisacrylamide (2,2-bis(acryloylamino)acetic acid, BAC) were employed. The latter was chosen to ascertain whether its acidic nature could favor the sorption of *o*-toluidine by establishing ionic interaction. With  $\gamma$ -CD, the same reaction succeeded only in the case of BAC, while BP failed to produce insoluble resins. Therefore, BAC- $\gamma$ -CD nanosponge was the only  $\gamma$ -CD-based one prepared.

For the sake of simplicity, Scheme 1 assumes that the polyaddition involved only the primary CD hydroxyl groups, neglecting the secondary ones. This, however, was not proven, and no reasonable predictions in this regard can be made. In fact, whereas the primary hydroxyl groups are less sterically hindered, the secondary ones are stronger acids, hence preferentially ionized (Loftsson and Brewster 1996). The bisacrylamide/CD molar ratio in the feed (Table 1) was adjusted to prepare nanosponges with maximum CD content, hence, presumably, maximum sorption capacities. As stated above, only BAC gave nanosponges with all three CDs, while BP failed in giving nanosponges with  $\gamma$ -CD. All nanosponges were purified by repeatedly soaking with water, then with ethanol, and finally dried to constant weight at 50 °C and 0.2 tor. Their

**Table 1** Elemental analyses and CD contents of BAC-CD and BP-CD nanosponges

Sample	C%		N %		Feed <sup>a</sup>	Bisacrylamide/CD (mmol mmol <sup>-1</sup> )		CD (mmol g <sup>-1</sup> nanosponge)
	Feed <sup>a</sup>	Found <sup>b</sup>	Feed <sup>a</sup>	Found <sup>b</sup>		Found <sup>b</sup>	Feed <sup>a</sup>	Found <sup>b</sup>
BAC- $\alpha$ -CD	46.17	42.42	6.03	4.82	3.66	2.54	0.59	0.68
BAC- $\beta$ -CD	45.75	42.12	5.11	4.03	3.25	2.29	0.56	0.63
BAC- $\gamma$ -CD	45.50	40.55	3.89	3.05	2.48	1.80	0.56	0.60
BP- $\alpha$ -CD	51.82	44.29	6.12	4.72	3.69	2.44	0.59	0.69
BP- $\beta$ -CD	50.32	44.13	4.88	3.96	2.56	2.21	0.61	0.64

<sup>a</sup>Feed: expected according to the preparation recipe

<sup>b</sup>Found: as determined from elemental analyses data

compositions, as determined by elemental analysis, are reported in Table 1. On the whole, the CD content of the resultant resins ranged between 0.60 mmol CD g<sup>-1</sup> and 0.69 mmol CD g<sup>-1</sup> nanosponge (67.0 wt% and 78.0 wt%) and, for all nanosponges, was higher than in the reactant mixtures, probably due to the loss of residual unreacted bisacrylamides or soluble CD/acrylamide oligomers. This loss was apparently slightly more pronounced for  $\alpha$ -CD-based nanosponges. The bisacrylamide moiety/CD molar ratio, calculated from elemental analyses data, ranged between 1.80 and 2.54. The lowest ratio was observed for BAC- $\gamma$ -CD, the only  $\gamma$ -CD resins obtained, while in all other cases, it was greater than 2.21. This result is in line with the higher water sorption of BAC- $\gamma$ -CD (see below), due to a lower crosslink extent of this nanosponge.

All nanosponges were characterized by FTIR spectroscopy. The spectra (Fig. 1) showed intense diagnostic bands typical of parent CDs and their addition products with either BAC or BP.

In particular, the characteristic -OH, -CH<sub>2</sub>, and C-O stretching bands of the CD patterns were observed at 3283

cm<sup>-1</sup>, 2924 cm<sup>-1</sup>, and 1024 cm<sup>-1</sup>, respectively. Meanwhile, in the BAC-based nanosponges, the diagnostic amide C=O stretching and NH bending bands of BAC addition residues were observed at 1616 cm<sup>-1</sup> and 1515 cm<sup>-1</sup>, respectively. The same bands for BP addition residues, with the exception of the NH bending bands of BAC, were observed at 1616 cm<sup>-1</sup> and 1436 cm<sup>-1</sup>. The -CH<sub>2</sub>- groups, present in all amide-deriving structural units, gave rise to the C-H stretching and bending bands observed at 2924 cm<sup>-1</sup> and 1380 cm<sup>-1</sup>, respectively. The broad band typical of the N-H amide stretching, expected at 3283 cm<sup>-1</sup> for BAC-deriving nanosponges, overlapped with the OH stretching band of CD.

All nanosponges were characterized by differential scanning calorimetry (DSC) and thermogravimetric analysis (TGA). The DSC traces of the second heating cycle following a cooling cycle carried out with the same rate (20 °C min<sup>-1</sup>) (Fig. 2) showed substantially flat curves in the 20–150 °C range, with no evidence of transition temperatures. The thermal decomposition onset was observed at temperatures higher than 200 °C, in line with previously

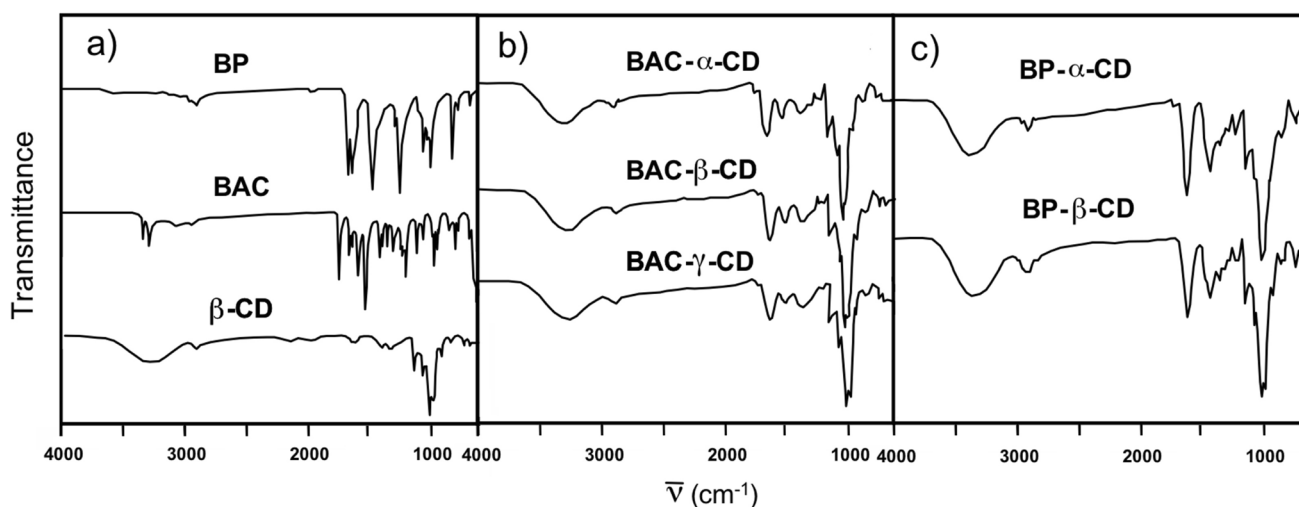
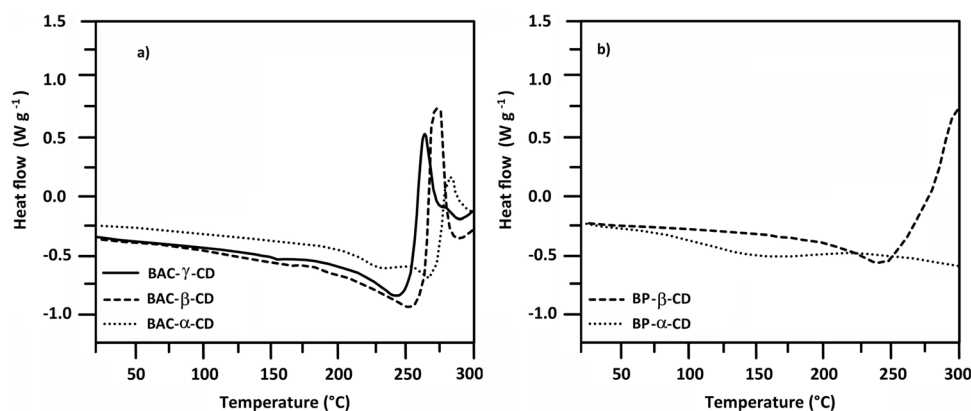


**Fig. 1** FTIR spectra of (a) native BP, BAC, and  $\beta$ -CD; (b) BAC-CD nanosponges; (c) BP-CD nanosponges

**Fig. 2** DSC thermograms of BAC-CD and BP-CD nanosponges. Heating rate: 20 °C min<sup>-1</sup>



published results obtained with differently crosslinked CD-based resins (Krause et al. 2010).

The thermal stability of BAC-CD and BP-CD nanosponges was compared with that of parent CDs, as shown by the TG traces displayed in Fig. 3 and by the collected data reported in Table 2. In line with previous observations on the thermal behavior of CD nanosponges obtained using different crosslinkers (Kumar et al. 2018; Salgin et al. 2017), the decomposition patterns of BAC-CD and BP-CD appeared to be far more complex than those of plain cyclodextrins.

In agreement with literature reports (Trotta et al. 2000), the TG curves of cyclodextrins had a similar three-stage profile, including (i) a first stage of dehydration, up to 120 °C, in which sorbed and crystallization water was removed; (ii) a second stage, from 250 to 350 °C, associated with a  $T_{\text{onset}10\%}$  around 300 °C, a maximum weight loss of 75–80% at  $T_{\text{max}1}$  332–333 °C, and the formation of a thermally stable residue, called char; and (iii) a third stage at temperatures above 400 °C in which char formed in the previous stage progressively degraded down to a residual mass fraction at 600 °C, RMF<sub>600</sub>, of 11.0–12.5%. The main decomposition phase centered at  $T_{\text{max}1}$  was attributed to the opening of the cyclodextrin ring, followed by structural transformations similar to those of cellulose, which include the loss of glycosidic and hydroxyl groups and the formation of double bonds, carbonyl groups, and aromatic structures.

The TG patterns of BAC-CD and BP-CD nanosponges exhibited  $T_{\text{onset}10\%}$  values invariably lower (Table 2) than those of cyclodextrins. Moreover, the weight loss patterns proceeded through four decomposition steps (Fig. 3) down to a significantly higher RMF<sub>600</sub> of 23.0–33.0%. In detail, apart from the dehydration stage, up to 120 °C, a second weight loss of approximately 5–15% occurred in the 150–300 °C range, ascribed to the cleavage of the C–C bond between CD and the linker. The third stage of degradation, ascribed to CD decomposition, was found at slightly different temperatures depending on the nature of the linker. All BAC-CD nanosponges had similar  $T_{\text{max}2}$ , around 345 °C, with a weight loss of around 45% in the range of 300–400 °C. Regarding

BP-CD nanosponges, BP-α-CD exhibited a  $T_{\text{max}2}$  value of 445 °C and BP-β-CD of 342 °C. The fourth step (400–600 °C and 500–600 °C for BAC- and BP-based cyclodextrins, respectively) was ascribed to the relatively slow thermal degradation of the char formed in the previous step.

The swelling ability of nanosponges was determined both in water and 0.01 M PBS pH 7.4. The results are shown in Fig. 4. The swelling in water was higher than in buffer and, for nanosponges with the same crosslinking arm, increased in the order α-CD < β-CD < γ-CD. The swelling degree is also influenced by the structure of the crosslinking arm. Under the same conditions, BAC nanosponges constantly swelled more than those based on the same CD, but deriving from BP, possibly due to the ionic nature of BAC.

### o-Toluidine sorption

The o-toluidine sorption ability of CD nanosponges was assessed by monitoring the o-toluidine depletion from 10<sup>-4</sup> M (about 10 ppm) aqueous solutions in linear sweep voltammetry experiments, making use of MWCNT-modified glassy carbon (GC) electrodes, a robust and sensitive analytical method that has proven to detect o-toluidine down to 0.16 ppm with an apparent recovery factor of about 100% (Pifferi et al. 2014). The sorption study was made at the natural pH in which o-toluidine is present in water-polluted samples. Moreover, the range of pollutant concentration investigated in this work was really low, thus not influencing the solution pH during the sorption.

The observed sorption capacities were compared with those of native soluble α-, β-, and γ-CDs. In all cases, the sorption kinetics, expressed both referring to the sorbent mass unit (Fig. 5a) and the molar CD content of the sorbent (Fig. 5b), were found to fit a mono-exponential kinetic model derived from a more conventional double-exponential model in which the second term prevails over the second one, indicating a good homogeneity of the sorbent materials (Ferruti et al. 2006), and the absence of adsorptive phenomena in competition with sorption.

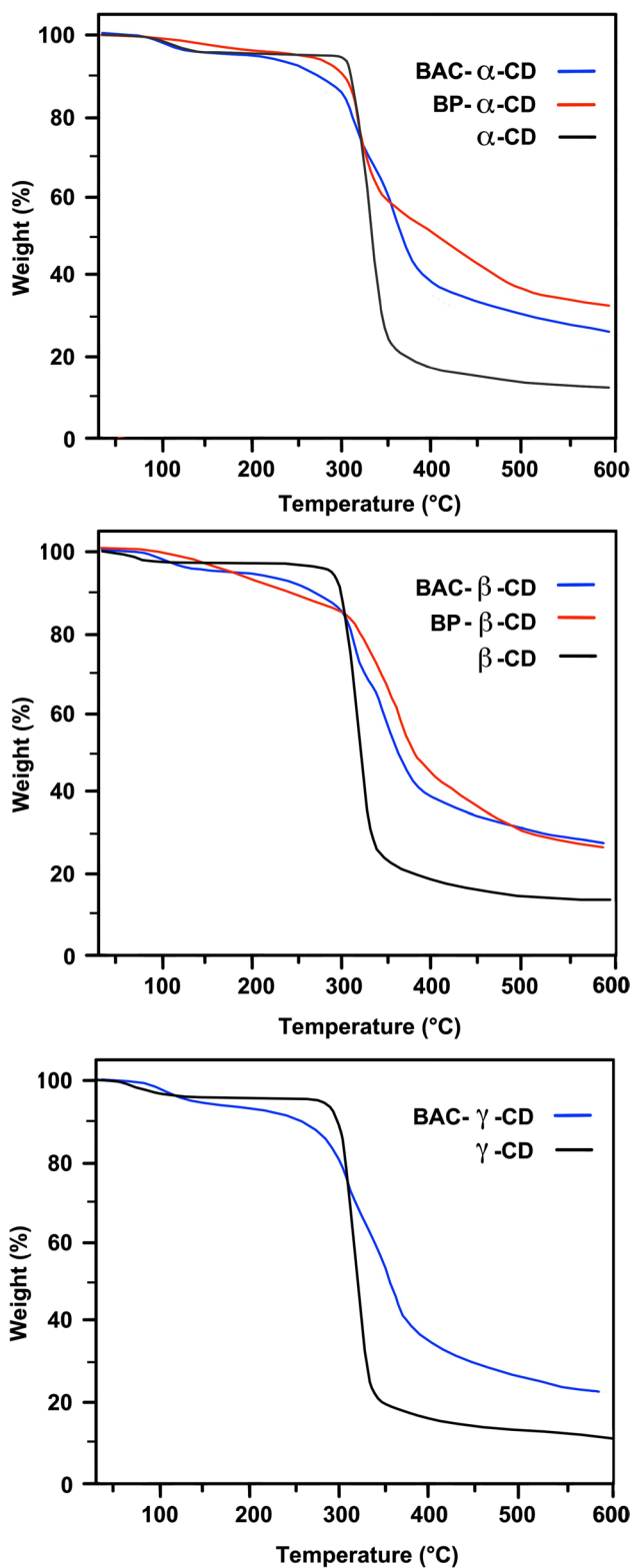


Fig. 3 TG traces of BAC-CD and BP-CD nanosponges obtained in nitrogen. Heating rate: 20 °C min<sup>-1</sup>.

Table 2 Thermal data collected by TG analyses in nitrogen

Sample	T <sub>onset10%</sub> <sup>a</sup> (°C)	T <sub>max1</sub> <sup>b</sup> (°C)	T <sub>max2</sub> <sup>b</sup> (°C)	RMF <sub>600</sub> <sup>d</sup> (%)
α-CD	306	333	-	11.5
β-CD	311	333	-	12.5
γ-CD	303	332	-	11.0
BAC-α-CD	292	296	348	30.0
BAC-β-CD	290	287	345	31.0
BAC-γ-CD	285	285	345	23.0
BP-α-CD	302	298	445	33.0
BP-β-CD	252	-	342	30.5

<sup>a</sup>Onset decomposition temperature at 10% weight loss

<sup>b</sup>Temperature at maximum weight loss rate for the 1st decomposition step

<sup>c</sup>Temperature at maximum weight loss rate for the 2nd decomposition step

<sup>d</sup>Residual mass fraction at 600 °C

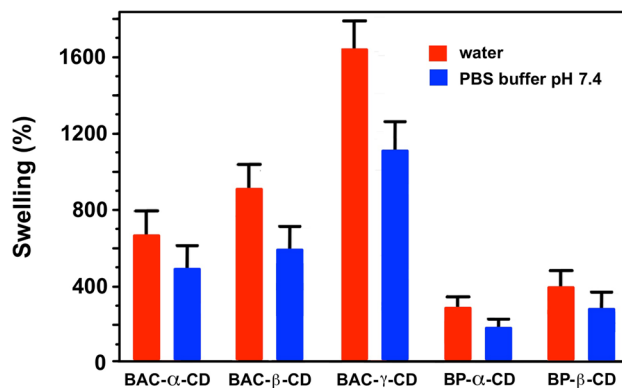


Fig. 4 Swelling behavior of BAC-CD and BP-CD nanosponges in water and PBS buffer pH 7.4

The mono-exponential model implies the following equations (Eqs. (2) and (3)):

$$q_t = q_e - \frac{D}{m_{\text{sorb}}} e^{-k_D t} \tag{2}$$

$$q_t' = q_e' - \frac{D'}{\mu\text{mol}_{\text{CD}}} e^{-k_D' t} \tag{3}$$

where  $m_{\text{sorb}}$  is the weight of the sample of the sorbing material,  $\mu\text{mol}_{\text{CD}}$  is the quantity of CD present in the sorbing material,  $k_D$  is the relevant sorption rate constant,  $q_e$  and  $q_e'$  are the equilibrium *o*-toluidine sorption capacities, and  $D$  and  $D'$  are further parameters modulating the sorption rate. The relevant kinetic parameters obtained for all tested samples are reported in Table 3.

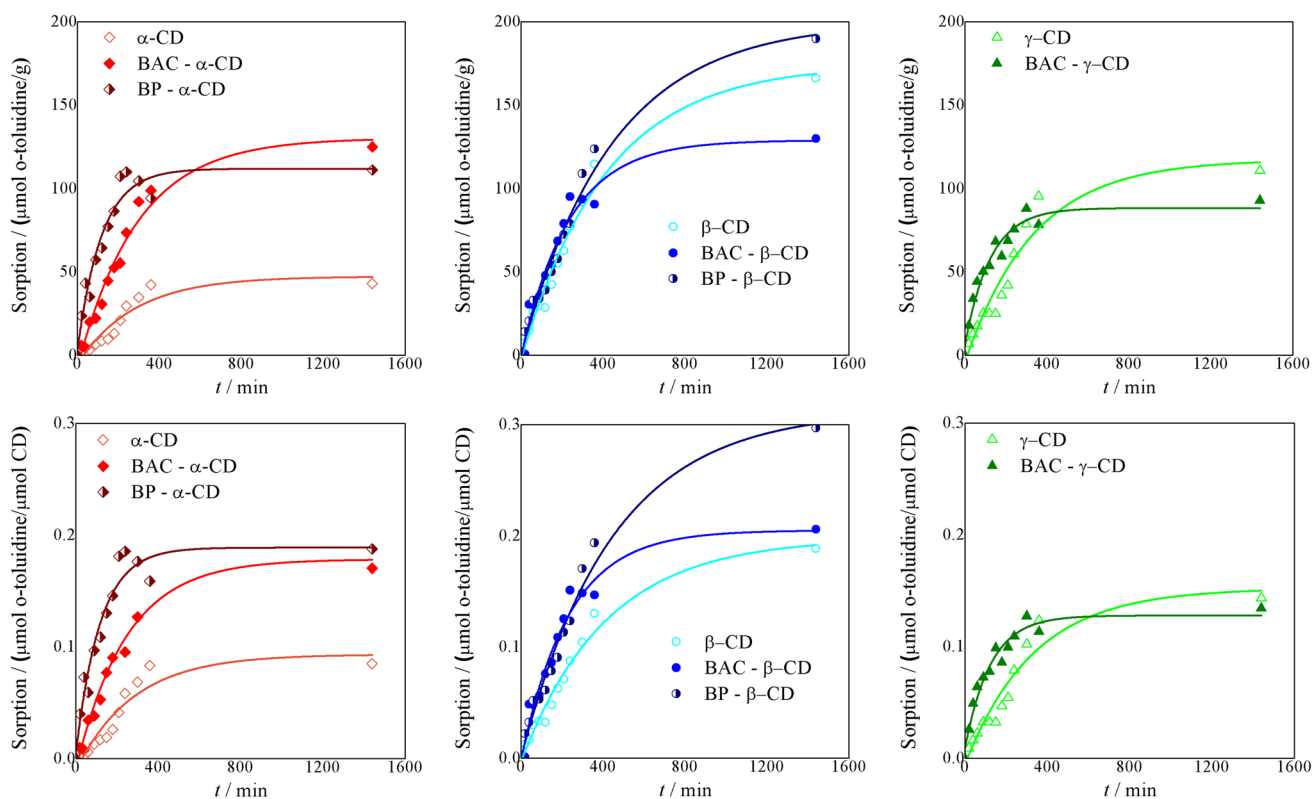


**Fig. 5** *o*-Toluidine sorption by soluble CDs, and CD-containing nanosponges referred to the CD (a) mass unit and (b) molar content in the sorbent [sorption experimental conditions: *o*-toluidine from an aque-

ous solution of  $10^{-4}$  M (10 ppm) in batch reactors under slight magnetic stirring]; corresponding mono-exponential kinetics in full lines

The sorption efficiency (see  $q_e$  and  $D$  values) of  $\beta$ -CD nanosponges is higher than that of  $\alpha$ -CD- and  $\gamma$ -CD- nanosponges in line with the higher efficiency of  $\beta$ -CD compared with that of both  $\alpha$ -CD and  $\gamma$ -CD, due to the specific capacity of the internal cavity size of  $\beta$ -CD to create stable inclusion complexes with monocyclic aromatic compounds (Szejtli 1998).

The equilibrium sorption capacities of both  $\alpha$ -CD and  $\beta$ -CD nanosponges, expressed as mol *o*-toluidine mol $^{-1}$  CD ( $q_e'$  factors, accounting for the number of sorption sites), were remarkably higher than those of parent cyclodextrins, particularly for  $\alpha$ -CD nanosponges. This was ascribed to two concurrent factors: the cooperation of correctly oriented cyclodextrin groups in forming inclusion complexes with *o*-toluidine and the additional uptake of *o*-toluidine

**Table 3** Experimental  $q_e$  values and kinetic parameters for the sorptions of *o*-toluidine from  $10^{-4}$  M (10 ppm) aqueous solutions by CD-based nanosponges [sorption experimental conditions: *o*-toluidine

from an aqueous solution of  $10^{-4}$  M (10 ppm) in batch reactors under slight magnetic stirring]

Sample	Sorption performance per g of sorbent			Sorption performance per $\mu\text{mol}$ of CD in the sorbent	
	$q_e$ ( $\mu\text{mol g}^{-1}$ )	$D$ ( $\mu\text{mol L}^{-1}$ )	$q_e'$ ( $\mu\text{mol } \mu\text{mol}^{-1}$ )	$D' \times 10^{-3}$ ( $\mu\text{mol L}^{-1}$ )	$k_D \times 10^{-3}$ ( $\text{min}^{-1}$ )
$\alpha$ -CD	$47 \pm 6$	$1.6 \pm 0.2$	$0.05 \pm 0.01$	$0.0031 \pm 0.0004$	$3.6 \pm 0.9$
BAC- $\alpha$ -CD	$104 \pm 7$	$3.5 \pm 0.2$	$0.15 \pm 0.01$	$0.0038 \pm 0.0002$	$4.1 \pm 0.6$
BP- $\alpha$ -CD	$112 \pm 7$	$3.0 \pm 0.2$	$0.16 \pm 0.01$	$0.0037 \pm 0.0003$	$8 \pm 2$
$\beta$ -CD	$174 \pm 9$	$5.3 \pm 0.3$	$0.20 \pm 0.01$	$0.0060 \pm 0.0003$	$2.4 \pm 0.3$
BAC- $\beta$ -CD	$137 \pm 5$	$4.2 \pm 0.2$	$0.24 \pm 0.01$	$0.0042 \pm 0.0002$	$3.4 \pm 0.3$
BP- $\beta$ -CD	$199 \pm 10$	$6.3 \pm 0.3$	$0.29 \pm 0.01$	$0.0062 \pm 0.0003$	$2.3 \pm 0.2$
$\gamma$ -CD	$117 \pm 11$	$3.6 \pm 0.3$	$0.15 \pm 0.01$	$0.0047 \pm 0.0005$	$3.0 \pm 0.6$
BAC- $\gamma$ -CD	$88 \pm 4$	$2.7 \pm 0.2$	$0.14 \pm 0.01$	$0.0024 \pm 0.0002$	$8 \pm 1$



by the interstitial channels created by the interconnected arms. On the opposite, the sorption capacity of BAC- $\gamma$ -CD was approximately the same as that of  $\gamma$ -CD. This could be attributed to the fact that due to the larger size of the internal cavity size of  $\gamma$ -CD and to the lower crosslinking degree that probably leads to wider interstitial channels in  $\gamma$ -CD nanosponges, *o*-toluidine complexation does not benefit from the establishment of cooperative effects between adjacent CD macrocycles.

It may also be observed that the BP-based nanosponges performed better than their BAC counterparts, more significantly in the case of BP- $\beta$ -CD. This behavior was ascribed to the higher affinity of the BP-deriving interconnecting arms for *o*-toluidine. The above-reported assumption that owing to its acidic nature, the BAC interconnecting arms could favor the sorption of *o*-toluidine by establishing ionic interactions did not materialize.

As regards *o*-toluidine removal from water, it is worth mentioning that the best results obtained in this work are significantly superior to those of other *o*-toluidine sorbents. In particular, the *o*-toluidine abatement dropped to 0.16 ppm, which represents the detection limit of the adopted analytical technique, lower by one order of magnitude than the figures reported so far for all other sorbents (Sun et al. 2010). In addition, all nanosponges, irrespective of the size of the CD inner cavity, proved capable of removing *o*-toluidine from dilute aqueous solutions under conditions similar to those usually found on the field in most *o*-toluidine-polluted aquifers, abating it down to at least 0.16 ppm. Remarkably, the fact that all three CDs lead to effective nanosponges allows us to conclude that high-performance *o*-toluidine sorbents can be prepared from commercially available crude CD blends, which are very cheap compared to pure samples of  $\alpha$ ,  $\beta$ , and  $\gamma$ -CD used in this pioneering work. This is of paramount importance in view of the mass production of CD-bisacrylamide nanosponges for water purification.

### Nanosponge regeneration

Regeneration studies were performed for BP- $\beta$ -CD, the sorbent with the highest *o*-toluidine equilibrium sorption. The nanosponge was simply regenerated by methanol extraction of the sorbed material. Three *o*-toluidine sorption-desorption cycles were performed. The sorption capacity after regeneration was monitored each time and compared with that of the pristine nanosponge. Interestingly, the sorption capacity (Fig. 6) slightly improved after the first regeneration treatment, possibly due to a rearrangement of the nanosponges network that facilitated the *o*-toluidine inclusion in a sort of imprinting of the polymer. More investigations should be done to prove this preliminary idea.

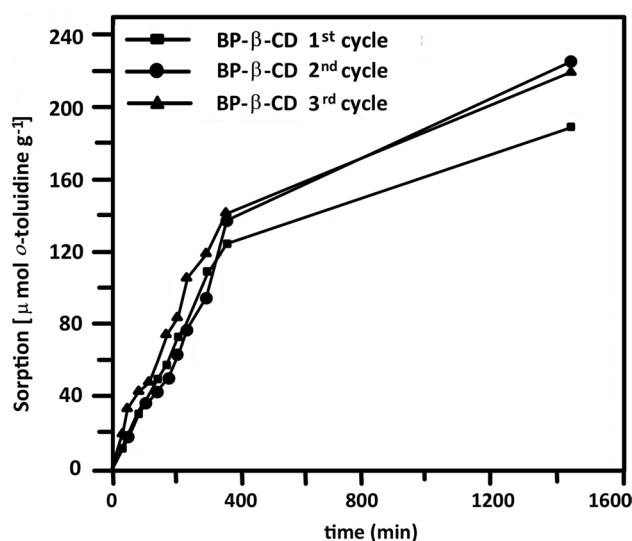


**Fig. 6** Sorption capacities of *o*-toluidine for BP- $\beta$ -CD nanosponges before (1st cycle) and after recycling (2nd and 3rd cycles)

### Conclusions

Tailor-made  $\alpha$ -,  $\beta$ -, and  $\gamma$ -CD-based nanosponges characterized by high CD content, in which the CD moieties were covalently connected by either ionizable or neutral bisacrylamide-deriving arms, were synthesized from cyclodextrins and bisacrylamides by base-catalyzed stepwise oxo-Michael polyaddition in aqueous solution. These nanosponges exhibited high water sorption ability and were thermally stable at least up to 250 °C. Their TG patterns significantly differed from those of the parent CD and were in line with those of previously reported CD nanosponges. These CD nanosponges removed *o*-toluidine from  $10^{-4}$  M ( $\sim 10$  ppm) aqueous solutions (the reference UK-approved maximum exposure limit) down to the detection limit of the adopted analytical technique (0.16 ppm).

The nanosponges' sorption capacities were in the range of 88–199  $\mu\text{mol g}^{-1}$  (10–21.3  $\text{mg g}^{-1}$ ), one order of magnitude higher with respect to other CD-containing sorbents reported in the literature (Sun et al. 2010). Interestingly, the sorption capacity of nanosponges toward *o*-toluidine was even higher than that of the corresponding cyclodextrins. This can be attributed to the participation in the sorption process of the interstitial channels between the CD units.

The sorbents were simply regenerated by extracting with methanol and recycled with no loss of performance. On the opposite, their sorption capacity slightly increased, possibly due to some molecular imprinting during the first sorption/desorption cycle. Also considering the simplicity, potential scalability (the preparation process can be extended to any compound containing two activated acrylamide double bonds (Ferruti et al. 2019)), environmental sustainability

of their preparation, and no phyto-toxicity (Alongi et al. 2022), these cyclodextrin-based materials warrant potential as *o*-toluidine sorbents competitive with most materials presented so far to the same purpose and deserve further investigations aimed at widening their scope as sorbents of organic water pollutants other than *o*-toluidine.

**Author contribution** Conceptualization, validation, investigation, methodology: all authors; formal analysis: V.P., E.F., A.M., and J.A.; writing – original draft: L.F., P.F., and E.R.; writing – review and editing: all authors; supervision, project administration, resources: L.F. and E.R.

**Funding** Open access funding provided by Università degli Studi di Milano within the CRUI-CARE Agreement.

**Data availability** The main data generated within this research are included in the paper. Some further data that support the findings are available from the corresponding author upon reasonable request.

## Declarations

**Ethics approval** This work does not contain any studies with human participants or animals.

**Consent to participate** All authors provided informed consent to participate in this research study.

**Consent for publication** The authors transfer to the journal the publication rights and guarantee that this contribution is original. All authors mutually agree on its submission.

**Competing interests** The authors declare no competing interests.

**Open Access** This article is licensed under a Creative Commons Attribution 4.0 International License, which permits use, sharing, adaptation, distribution and reproduction in any medium or format, as long as you give appropriate credit to the original author(s) and the source, provide a link to the Creative Commons licence, and indicate if changes were made. The images or other third party material in this article are included in the article's Creative Commons licence, unless indicated otherwise in a credit line to the material. If material is not included in the article's Creative Commons licence and your intended use is not permitted by statutory regulation or exceeds the permitted use, you will need to obtain permission directly from the copyright holder. To view a copy of this licence, visit <http://creativecommons.org/licenses/by/4.0/>.

## References

- Ahmed RZ, Patil G, Zaheer Z (2013) Nanosponges – a completely new nano-horizon: pharmaceutical applications and recent advances. *Drug Dev Ind Pharm* 39:1263–1272. <https://doi.org/10.3109/03639045.2012.694610>
- Allabashi R, Arkas M, Hörmann G, Tsiourvas D (2007) Removal of some organic pollutants in water employing ceramic membranes impregnated with cross-linked silylated dendritic and cyclodextrin polymers. *Water Res* 41:476–486. <https://doi.org/10.1016/j.watres.2006.10.011>
- Alongi J, Costantini A, Ferruti P, Ranucci E (2022) Evaluation of the eco-compatibility of polyamidoamines by means of seed germination test. *Polym Degrad Stab* 167:109854. <https://doi.org/10.1016/j.polymdegradstab.2022.109854>
- Anotai J, Thuptimrang P, Su CC, Lu MC (2011) Degradation of *o*-toluidine by fluidized-bed Fenton process: statistical and kinetic study. *Environ Sci Pollut Res Int* 19:169–176. <https://doi.org/10.1007/s11356-011-0553-x>
- Ansari KA, Vavia PR, Trotta F, Cavalli R (2011) Cyclodextrin-based nanosponges for delivery of resveratrol: in vitro characterisation, stability, cytotoxicity and permeation study. *AAPS PharmSciTech* 12:279–286. <https://doi.org/10.1208/s12249-011-9584-3>
- Baan R, Straif K, Grosse Y, Secretan B, El Ghissassi F, Bouvard V, Benbrahim-Tallaa L, Coglianò V (2008) Carcinogenicity of some aromatic amines, organic dyes, and related exposures. *Lancet Oncol* 9:322–323. [https://doi.org/10.1016/S1470-2045\(08\)70089-5](https://doi.org/10.1016/S1470-2045(08)70089-5)
- Berto S, Bruzzoniti MC, Cavalli R, Perrachon D, Prenesti E, Sarzanini C, Trotta F, Tumiatti W (2007a) Synthesis of new ionic  $\beta$ -cyclodextrin polymers and characterization of their heavy metals retention. *J Incl Phenom Macrocyc Chem* 57:631–636. <https://doi.org/10.1007/s10847-006-9273-0>
- Berto S, Bruzzoniti MC, Cavalli R, Perrachon D, Prenesti E, Sarzanini C, Trotta F, Tumiatti W (2007b) Highly crosslinked ionic  $\beta$ -cyclodextrin polymers and their interaction with heavy metals. *J Incl Phenom Macrocyc Chem* 57:637–643. <https://doi.org/10.1007/s10847-006-9270-3>
- Bilensoy E (2011) Cyclodextrins in pharmaceuticals, cosmetics, and biomedicine. John Wiley & Sons, Hoboken
- Bishop PL, Uribe A, Pinto NG (2002) The influence of pH and temperature changes on the adsorption behavior of organophilic clays used in the stabilization/solidification of hazardous wastes. *J Environ Eng Sci* 1:123–133. <https://doi.org/10.1139/s02-007>
- Cappelletti G, Pifferi V, Mostoni S, Falciola L, Di Bari C, Spadavecchia F, Meroni D, Davoli E, Ardizzone S (2015) Hazardous *o*-toluidine mineralization by photocatalytic bismuth doped ZnO slurries. *Chem Commun* 51:10459–10462. <https://doi.org/10.1039/C5CC02620B>
- Cavalli R, Akhter AK, Bisazza A, Giustetto P, Trotta F, Vavia P (2010) Nanosponge formulations as oxygen delivery systems. *Int J Pharm* 402:254–257. <https://doi.org/10.1016/j.ijpharm.2010.09.025>
- Crini G (2005) Recent developments in polysaccharide-based materials used as adsorbents in wastewater treatment. *Prog Polym Sci* 30:38–70. <https://doi.org/10.1016/j.progpolymsci.2004.11.002>
- Crini G, Janus L, Morcellet M, Torri G, Morin N (1999) Sorption properties toward substituted phenolic derivatives in water using macroporous polyamines containing  $\beta$ -cyclodextrin. *J Appl Polym Sci* 73:2903–2910. [https://doi.org/10.1002/\(SICI\)1097-4628\(19990929\)73:14%3c2903::AID-APP14%3e3.0.CO;2-2](https://doi.org/10.1002/(SICI)1097-4628(19990929)73:14%3c2903::AID-APP14%3e3.0.CO;2-2)
- Dodziuk H (2006) Cyclodextrins and their complexes: chemistry, analytical methods. Applications. Wiley-VCH Verlag GmbH & Co. KGaA, Weinheim
- Duman O, Ayranci E (2005) Structural and ionization effects on the adsorption behaviors of some anilinic compounds from aqueous solution onto high-area carbon-cloth. *J Hazard Mater* 120:173–181. <https://doi.org/10.1016/j.jhazmat.2004.12.030>
- Elgarahy AM, Elwakeel KZ, Mohammad SH, Elshoubaky GA (2021) A critical review of biosorption of dyes, heavy metals and metalloids from wastewater as an efficient and green process. *Cleaner Engineering and Technology* 4:100209. <https://doi.org/10.1016/j.clet.2021.100209>
- El-Sayed WN, Elwakeel KZ, Shahat A, Awual MR (2019) Investigation of novel nanomaterial for the removal of toxic substances from contaminated water. *RSC Adv* 9:14167–14175. <https://doi.org/10.1039/C9RA00383E>

- Essington ME (1994) Adsorption of aniline and toluidines on montmorillonite. *Soil Sci* 158:181–188. <https://doi.org/10.1097/00010694-199409000-00004>
- Fan Y, Feng YQ, Da SL (2003) On-line selective solid-phase extraction of 4-nitrophenol with  $\beta$ -cyclodextrin bonded silica. *Anal Chim Acta* 484:145–153. [https://doi.org/10.1016/S0003-2670\(03\)00342-8](https://doi.org/10.1016/S0003-2670(03)00342-8)
- Faraji H, Husain SW, Helalizadeh M (2011)  $\beta$ -cyclodextrin-bonded silica particles as novel sorbent for stir bar sorptive extraction of phenolic compounds. *J Chromatogr Sci* 49:482–487. <https://doi.org/10.1093/chrsi/49.6.482>
- Ferruti F, Alongi J, Manfredi A, Ranucci E, Ferruti P (2019) Controlled synthesis of linear polyamidoamino acids. *Polymers* 11:1324. <https://doi.org/10.3390/polym11081324>
- Ferruti P (1985) Poly (amido-amine)s. *Macromol Synth* 9:25–29
- Ferruti P, Ranucci E, Trotta F, Gianasi E, Evagorou EG, Wasil M, Wilson G, Duncan R (1999) Synthesis, characterisation and antitumour activity of platinum (II) complexes of novel functionalised poly (amido amine)s. *Macromol Chem Phys* 200:1644–1654. [https://doi.org/10.1002/\(SICI\)1521-3935\(19990701\)200:7%3c1644::AID-MACP1644%3e3.0.CO;2-P](https://doi.org/10.1002/(SICI)1521-3935(19990701)200:7%3c1644::AID-MACP1644%3e3.0.CO;2-P)
- Ferruti P, Ranucci E, Bianchi S, Falciola L, Mussini PR, Rossi M (2006) Novel polyamidoamine-based hydrogel with an innovative molecular architecture as  $\text{Co}^{2+}$ -,  $\text{Ni}^{2+}$ -, and  $\text{Cu}^{2+}$ -sorbing material: cyclic voltammetry and extended X-ray absorption fine structure studies. *J Polym Sci Part A Polym Chem* 44:2316–2327. <https://doi.org/10.1002/POLA.21349>
- García-Zubiri IX, González-Gaitano G, Isasi JR (2007) Isothermic heats of sorption of 1-naphthol and phenol from aqueous solutions by  $\beta$ -cyclodextrin polymers. *J Colloid Interface Sci* 307:64–70. <https://doi.org/10.1016/j.jcis.2006.10.076>
- Gregg N, Dobson S, Cary R (1998) o-Toluidine. World Health Organization & International Programme on Chemical Safety. World Health Organization. <https://apps.who.int/iris/handle/10665/42040>
- Gupta VK, Nayak A, Agarwal S (2012) Performance evaluation and application of oxygen enriched waste rubber tire adsorbent for the removal of hazardous aniline derivatives from waste water. *Chem Eng J* 203:447–457. <https://doi.org/10.1016/j.cej.2012.07.051>
- Janus L, Crini G, El-Rezzi V, Morcellet M, Cambiaghi A, Torri G, Naggi A, Vecchi C (1999) New sorbents containing beta-cyclodextrin. Synthesis, characterization and sorption properties. *React Funct Polym* 42:173–180. [https://doi.org/10.1016/S1381-5148\(98\)00066-2](https://doi.org/10.1016/S1381-5148(98)00066-2)
- Jianguo C, Aimin L, Hongyan S, Zhenghao F, Chao L, Quanxing Z (2005) Adsorption characteristics of aniline and 4-methylaniline onto bifunctional polymeric adsorbent modified by sulfonic groups. *J Hazard Mater* 124:173–180. <https://doi.org/10.1016/j.jhazmat.2005.05.001>
- Krubicov I, Appleton SL, Tannous M, Hoti G, Caldera F, Pedrazzo AR, Cecone C, Cavalli R, Trotta F (2020) History of Cyclodextrin Nanosponges *Polymers* 12:1122. <https://doi.org/10.3390/polym12051122>
- Krause RWM, Mamba BB, Bambo FM, Malefetse TJ (2010) Cyclodextrin polymers: Synthesis and application in water treatment. In: Hu J (ed) *Cyclodextrins: Chemistry and Physics*. Transworld Research Network, Kerala, India
- Kumar S, Sihag P, Trotta F, Rao R (2018) Encapsulation of Babchi oil in cyclodextrin-based nanosponges: physicochemical characterization, photodegradation, and in vitro cytotoxicity studies. *Pharmaceutics* 10:169. <https://doi.org/10.3390/pharmaceutics10040169>
- Li D, Ma M (1999) Nanosponges: from inclusion chemistry to water purifying technology. *ChemTech* 29:31–37
- Liu Z, Yang H, Huang Z, Zhou P, Liu SJ (2002) Degradation of aniline by newly isolated, extremely aniline-tolerant *Delftia sp.* AN3. *Appl Microbiol Biotechnol* 58:679–682. <https://doi.org/10.1007/s00253-002-0933-8>
- Loftsson T, Brewster M (1996) Pharmaceutical applications of cyclodextrins. 1. Drug solubilization and stabilization. *J Pharm Sci* 85:1017–1025. <https://doi.org/10.1021/js950534b>
- López-Grimau V, Riera-Torres M, López-Mesas M, Gutiérrez-Bouzán C (2013) Removal of aromatic amines and decolourisation of azo dye baths by electrochemical treatment. *Color Technol* 129:267–273. <https://doi.org/10.1111/cote.12021>
- Mardegan A, Pifferi V, Pontoglio E, Falciola L, Scopece P, Moretto LM (2014) Sprayed carbon nanotubes on pyrolysed photoresist carbon electrodes: application to o-toluidine determination. *Electrochem Commun* 48:13–16. <https://doi.org/10.1016/j.elecom.2014.08.004>
- Mhlanga SD, Mamba BB, Krause RW, Malefetse TJ (2007) Removal of organic contaminants from water using nanosponge cyclodextrin polyurethanes. *J Chem Technol Biotechnol* 82:382–388. <https://doi.org/10.1002/jctb.1681>
- Mognetti B, Barberis A, Marino S, Berta G, De Francia S, Trotta F, Cavalli R (2021) In vitro enhancement of anticancer activity of paclitaxel by a Cremophor free cyclodextrin-based nanosponge formulation. *J Incl Phenom Macrocycl Chem* 74:201–210. <https://doi.org/10.1007/s10847-011-0101-9>
- OECD, Organisation for Economic Co-operation and Development (2004) o-Toluidine – SIDS Initial Assessment Report for SIAM 19. United Nations Environment Programme (UNEP) Publications
- Petitjean M, García-Zubiri IX, Isasi JR (2021) History of cyclodextrin-based polymers in food and pharmacy: a review. *Environ Chem Lett* 19:3465–3476. <https://doi.org/10.1007/s10311-021-01244-5>
- Pifferi V, Cappelletti G, Ardizzone S, Falciola L, Di Bari C, Spadavecchia F, Meroni D, Carrà A, Cerrato G, Morandi S, Davoli E (2015) Photo-mineralization of noxious o-toluidine water pollutant by nano-ZnO: the role of the oxide surface texture on the kinetic path. *Appl Catal B Environ* 178:233–240. <https://doi.org/10.1016/j.apcatb.2014.08.043>
- Pifferi V, Cappelletti G, Di Bari C, Meroni D, Spadavecchia F, Falciola L (2014) Multi-walled carbon nanotubes (MWCNTs) modified electrodes: effect of purification and functionalization on the electroanalytical performances. *Electrochim Acta* 146:403–410. <https://doi.org/10.1016/j.electacta.2014.09.099>
- Rizzi V, Gubitosa J, Signorile R, Fini P, Cecone C, Matencio A, Trotta F, Cosma P (2021) Cyclodextrin nanosponges as adsorbent material to remove hazardous pollutants from water: the case of ciprofloxacin. *Chem Eng J* 411:128514. <https://doi.org/10.1016/j.cej.2021.128514>
- Romo A, Peñas FJ, Isasi JR, García-Zubiri IX, González-Gaitano G (2008) Extraction of phenols from aqueous solutions by  $\beta$ -cyclodextrin polymers. Comparison of sorptive capacities with other sorbents. *React Funct Polym* 68:406–413. <https://doi.org/10.1016/j.reactfunctpolym.2007.07.005>
- Salgin S, Salgin U, Vatansever Ö (2017) Synthesis and characterization of  $\beta$ -cyclodextrin nanosponge and its application for the removal of p-nitrophenol from water. *CLEAN - Soil Air Water* 45:1–10. <https://doi.org/10.1002/clen.201500837>
- San N, Çınar Z (2016) Structure-activity relations for the photodegradation reactions of monosubstituted anilines in  $\text{TiO}_2$  suspensions. *J Adv Oxid Technol* 5:85–92. <https://doi.org/10.1515/jaots-2002-0111>
- Sherje AP, Dravyakar BR, Kadam D, Jadhav M (2017) Cyclodextrin-based nanosponges: a critical review. *Carbohydr Polym* 173:37–49. <https://doi.org/10.1016/j.carbpol.2017.05.086>
- Sun ZY, Shen MX, Cao GP, Deng J, Liu Y, Liu T, Zhao L, Yuan WK (2010) Preparation of bimodal porous copolymer containing  $\beta$ -cyclodextrin and its inclusion adsorption behavior. *J Appl Polym Sci* 118:2176–2185. <https://doi.org/10.1002/app.32515>

- Swaminathan S, Cavalli R, Trotta F, Ferruti P, Ranucci E, Gerges I, Manfredi A, Marinotto D, Vavia PR (2010) In vitro release modulation and conformational stabilization of a model protein using swellable polyamidoamine nanospheres of  $\beta$ -cyclodextrin. *J Incl Phenom Macrocycl Chem* 68:183–191. <https://doi.org/10.1007/s10847-010-9765-9>
- Swaminathan S, Vavia PR, Trotta F, Cavalli R (2013) Nanospheres encapsulating dexamethasone for ocular delivery: formulation design, physicochemical characterization, safety and corneal permeability assessment. *J Biomed Nanotechnol* 9:998–1007. <https://doi.org/10.1166/jbn.2013.1594>
- Szejtli J (1998) Introduction and general overview of cyclodextrin chemistry. *Chem Rev* 98:1743–1753. <https://doi.org/10.1021/cr970022c>
- Taka AL, Pillay K, Mbianda XY (2017) Nanosphere cyclodextrin polyurethanes and their modification with nanomaterials for the removal of pollutants from waste water: a review. *Carbohydr Polym* 159:94–107. <https://doi.org/10.1016/j.carbpol.2016.12.027>
- Titus E, Kalkar AK, Gaikar VG (2002) Adsorption of anilines and cresols on NaX and different cation exchanged zeolites (equilibrium, kinetic, and IR investigations). *Sep Sci Technol* 37:105–125. <https://doi.org/10.1081/SS-120000324>
- Trotta F (2011) Cyclodextrin nanospheres and their applications. In Bilensoy E (ed) *Cyclodextrins in pharmaceuticals, cosmetics and biomedicine: current and future industrial applications*, John Wiley & Sons, Hoboken, pp 323–342. <https://doi.org/10.1002/9780470926819.ch17>
- Trotta F, Zanetti M, Camino G (2000) Thermal degradation of cyclodextrins. *Polym Degrad Stab* 69:373–379. [https://doi.org/10.1016/S0141-3910\(00\)00084-7](https://doi.org/10.1016/S0141-3910(00)00084-7)
- Trotta F, Zanetti M, Cavalli R (2012) Cyclodextrin-based nanospheres as drug carriers. *Beilstein J Org Chem* 8:2091–2099. <https://doi.org/10.3762/bjoc.8.235>
- Varana C, Anceschi A, Sevli S, Bruni N, Giraudo L, Bilgi E, Korkusuz P, İskit AB, Bilensoy E (2020) Preparation and characterization of cyclodextrin nanospheres for organic toxic molecule removal. *Int J Pharm* 585:119485. <https://doi.org/10.1016/j.ijpharm.2020.119485>
- Voumard P, Zhan Q, Zenobi R (1995) Adsorption of monosubstituted benzenes on low surface area silica studied by temperature programmed desorption and laser-induced thermal desorption methods. *Langmuir* 11:842–848. <https://doi.org/10.1021/la00003a027>
- Wilson LD, Mohamed MH, Berhaut CL (2011) Sorption of aromatic compounds with copolymer sorbent materials containing  $\beta$ -cyclodextrin. *Materials* 4:1528–1542. <https://doi.org/10.3390/ma4091528>
- Yadav M, Thakore S, Jadeja R (2022) A review on remediation technologies using functionalized cyclodextrin. *Environ Sci Pollut Res* 29:236–250. <https://doi.org/10.1007/s11356-021-15887-y>
- Yamasaki H, Makihata Y, Fukunaga K (2006) Efficient phenol removal of wastewater from phenolic resin plants using crosslinked cyclodextrin particles. *J Chem Technol Biotechnol* 81:1271–1276. <https://doi.org/10.1002/jctb.1545>
- Yu JC, Jiang ZT, Liu HY, Yu J, Zhang L (2003)  $\beta$ -Cyclodextrin epichlorohydrin copolymer as a solid-phase extraction adsorbent for aromatic compounds in water samples. *Anal Chim Acta* 477:93–101. [https://doi.org/10.1016/S0003-2670\(02\)01411-3](https://doi.org/10.1016/S0003-2670(02)01411-3)
- Zhang PC, Sparks DL (1993) Kinetics of phenol and aniline adsorption and desorption on an organo-clay. *Soil Sci Soc Am J* 57:340–345. <https://doi.org/10.2136/sssaj1993.03615995005700020009x>

**Publisher's note** Springer Nature remains neutral with regard to jurisdictional claims in published maps and institutional affiliations.